***Submitted to Engineering Geology***

# Reliability Sensitivity Analysis of Geotechnical Monitoring Variables Using Bayesian Updating

**Dian-Qing Li,** State Key Laboratory of Water Resources and Hydropower Engineering Science, Institute of Engineering Risk and Disaster Prevention, Wuhan University; 8 Donghu South Road, Wuhan 430072, P. R. China. Email: dianqing@whu.edu.cn

**Fu-Ping Zhang,** State Key Laboratory of Water Resources and Hydropower Engineering Science, Institute of Engineering Risk and Disaster Prevention, Wuhan University; 8 Donghu South Road, Wuhan 430072, P. R. China. Email: fupingzhang@whu.edu.cn

**Zi-Jun Cao,** State Key Laboratory of Water Resources and Hydropower Engineering Science, Institute of Engineering Risk and Disaster Prevention, Wuhan University; 8 Donghu South Road, Wuhan 430072, P. R. China. Email: zijuncao@whu.edu.cn

**Xiao-Song Tang,** State Key Laboratory of Water Resources and Hydropower Engineering Science, Institute of Engineering Risk and Disaster Prevention, Wuhan University; 8 Donghu South Road, Wuhan 430072, P. R. China. Email: xstang@whu.edu.cn

**Siu-Kui Au,** Institute for Risk and Uncertainty, University of Liverpool; Harrison Hughes Building, Brownlow Hill, Liverpool, L69 3GH, United Kingdom. Email: siukuiau@liverpool.ac.uk

Corresponding author: **Zi-Jun Cao**

Tel: (86)-27-6877 4036

Fax: (86)-27-6877 4295

E-mail: zijuncao@whu.edu.cn

## Abstract

Determining the sensitivity of monitoring variables is essential to field monitoring design for effectively monitoring the safety and reliability levels of geotechnical structures in uncertain environment. Reliability sensitivity analysis of monitoring variables provides a rational approach for identifying sensitive monitoring variables and is capable of accounting for geotechnical uncertainties. It, however, can be computationally expensive, especially when sophisticated numerical models (e.g., finite difference model, FDM) are involved and repeated simulation runs are required. This paper proposes a reliability sensitivity analysis method that leverages on the robustness of direct Monte Carlo simulation (MCS) and the Bayesian Updating with Structural Reliability Methods. The proposed approach allows performing the reliability sensitivity analysis of a monitoring variable by a single run of direct MCS, avoiding repeated simulation runs for different possible observational values of a given monitoring variable. Illustrative examples demonstrate the capability of the proposed approach in identifying the most sensitive monitoring variables among candidates. It is possible to achieve a significant reduction in the number of evaluations of numerical models for reliability sensitivity analysis of monitoring variables using the proposed approach.

**Keywords:** Monitoring design; Reliability analysis; Bayesian updating; Direct Monte Carlo simulation

## 1 Introduction

Geotechnical structures are frequently constructed and operated in highly uncertain environments due to the variability of load conditions and geo-materials that are affected by various geological processes and have undergone complex geological histories. For safety control and risk mitigation, field monitoring can be adopted in the field of engineering geology and geotechnical engineering to acquire information (e.g., displacement and groundwater level) reflecting safety and reliability levels of geotechnical structures by in-situ instrumentation (Juang et al., 2013; Schweckendiek and Vrouwenvelder, 2013; Peng et al., 2014; Yu et al., 2014; Kelly and Huang, 2015; Zhang et al., 2015; Camós et al., 2016; Ering and Babu, 2016; Li et al., 2016c, d; Hong et al., 2017; Xu et al., 2018; Zheng et al., 2018). Proper instrumentation is crucial to cost-effective field monitoring and rational assessment of geotechnical safety and reliability, which is usually accomplished through monitoring design. Monitoring design aims at identifying monitoring variables sensitive to the safety and reliability level of the subject geotechnical structure amidst various geotechnical uncertainties (such as those in soil/rock parameters and loads).

Reliability sensitivity analysis (Au, 2005; Sudret, 2008; Wang, 2012) provides a rigorous and rational framework for identifying sensitive monitoring variables from a pool of candidates (e.g., displacements at different locations of a slope). Under a reliability sensitivity analysis framework, the sensitivity of the reliability of a geotechnical system (e.g., slope) to a monitoring variable $Z$ can be quantitatively reflected by the variation of failure probability, $P_F$, of the geotechnical system as a function of $Z$, which is referred to as the 'failure probability function' (FPF) with respect to the monitoring variable (i.e., FPFwMV) in this study.

Determining FPFwMV for the monitoring design, during which no monitoring information has been obtained, requires one to calculate $P_F$ for different prescribed values of the monitoring variable concerned. This is a nontrivial task at least for two reasons. First, the monitoring variable (e.g., displacements at some locations of a slope) may not be identical to the design performance (e.g., safety factor of slope stability, $FS$) of geotechnical structures, and they are usually linked through mathematical models, such as finite element model (FEM) and finite difference model (FDM), in an implicit and indirect manner. For practical applications, the model can be very complex and its evaluation is a computationally expensive task. Second, incorporating the monitoring information into evaluation of $P_F$ is frequently performed under a Bayesian framework, in which the probability distribution of $\mathbf{x}$ is updated based on monitoring information and $P_F$ is re-evaluated using the updated probability distribution (e.g., Hsiao et al., 2008; Straub, 2011; Papaioannou and Straub, 2012; Schweckendiek and Vrouwenvelder, 2013; Wang et al., 2012; Zhang et al., 2013; Peng et al., 2014; Li et al., 2016 b, c, d). By this means, determining FPFwMV often necessitates repeated Bayesian analyses and reliability assessments of geotechnical structures for different values of the monitoring variable concerned. This can be computationally prohibitive as complex models are involved.

The above computational difficulty becomes more profound as the FPFwMV is evaluated through simulation-based methods that are generally applicable to complex models, such as Monte Carlo simulation (MCS) (e.g., Ang and Tang, 2007; Zhang et al., 2014, 2017; Li et al., 2015; Gong et al., 2017, 2018; Xiao et al., 2018; Qi and Li, 2018), Markov Chain Monte Carlo simulation (MCMCS) (e.g., Zhang et al., 2010, 2012; Wang and Cao, 2013; Cao and Wang, 2014), and Subset simulation (e.g., Au and Wang, 2014; Li et al., 2016a; Xiao et al., 2016; Jiang et al., 2018). Previous studies (e.g., Au, 2005; Ching and Hsieh, 2007; Wang et al., 2010; Wang, 2012; Yuan, 2013; Li et al., 2015) have developed several MCS-based methods for efficient reliability sensitivity analyses. These methods provide the reliability sensitivity on uncertain model parameters $\mathbf{x}$ (e.g., shear strength parameters) or design geometry parameters (e.g., slope height and angle), which are directly used as input to evaluate the design performance (e.g., *FS*) concerned. However, how to make use of MCS methods (e.g., direct MCS) to efficiently evaluate the reliability sensitivity of geotechnical structures with respect to monitoring variables, which are often implicit functions of $\mathbf{x}$, remains an open question.

This paper develops a MCS-based method for reliability sensitivity analysis of monitoring variables for geotechnical structures, which leverages on the robustness of direct Monte Carlo simulation (MCS) and the recently established analogy between reliability and Bayesian updating problem, i.e., the BUS (Bayesian Updating with Structural Reliability Methods) framework (Straub and Papaioannou 2015). The proposed approach evaluates the FPFwMV by a single run of direct MCS, avoiding repeated simulation runs for different possible observational values of a given monitoring variable. This allows performing reliability sensitivity analysis for identifying sensitive monitoring variables with complex computational models, which accounts for various geological factors (e.g., geological discontinuities) in a more detailed and realistic manner for the real world engineering problems, prior to the monitoring. Moreover, if observational data are obtained during the monitoring, the updated reliability of geotechnical structure concerned can be directly read from the FPFwMV for real-time risk-based decision making, which is a nontrivial task because the posterior reliability analysis is often involved. The paper starts with the description of a general framework for reliability sensitivity analysis of monitoring variables, followed by development of the proposed approach. To improve the accuracy of the estimated FPFwMV, a modified rejection sampling principle is also developed. Finally, the proposed approach is illustrated using two geotechnical monitoring examples.

## 2 General framework for reliability sensitivity analysis of monitoring variables

Consider a geotechnical environment where one wants to determine a set of quantities for monitoring purpose. Fig.1 illustrates schematically the proposed reliability sensitivity analysis framework for monitoring variables. It starts with determining a number, $M$, of candidate monitoring variables $Z_k$ ($k = 1, 2, \dots, M$) (e.g., displacements and groundwater level) based on site conditions and equipment availability. To effectively monitor the change in the reliability level of geotechnical structures (e.g., levee and slope), one needs to identify sensitive monitoring variables to guide in-situ instrumentation, which can be achieved by comparing the FPFs of candidate monitoring variables. For a given monitoring variable $Z_k$, the corresponding FPF is obtained by calculating failure probabilities $P_F(Z_k = z_{k,l})$ of the geotechnical structure at a number, $N_k$, of possible observational values (POVs), $z_{k,l}$, $l = 1, 2, \dots, N_k$, of $Z_k$. Herein, failure is defined in terms of the design performance (e.g., $FS$ of slope stability) of the geotechnical structure, which need not be the same as the monitoring variables. Note that, at the instrumentation design stage, monitoring information is not available, and some POVs of monitoring variables are prescribed for the reliability sensitivity analysis. For a given POV $z_{k,l}$ of $Z_k$, its corresponding $P_F$ ($Z_k = z_{k,l}$) can be calculated through two steps: (1) determine the conditional probability distribution of uncertain model parameters $\mathbf{x}$, which are directly used to evaluate the geotechnical design performance, given $Z_k = z_{k,l}$; and (2) evaluate $P_F$ ($Z_k = z_{k,l}$) based on the conditional probability distribution of $\mathbf{x}$, which are provided as below.

Using the Bayes' Theorem, the conditional probability density function (PDF) $f(\mathbf{x}|z_{k,l})$ of $\mathbf{x}$ given $Z_k = z_{k,l}$, often referred as the 'posterior PDF', can be expressed as:

$$f(\mathbf{x}|z_{k,l}) = f(z_{k,l}|\mathbf{x})f(\mathbf{x})/f(z_{k,l}) \quad \text{for } k = 1, 2, \ldots, M \text{ and } l = 1, 2, \ldots, N_k \tag{1}$$

where $f(\mathbf{x})$ is the prior PDF of $\mathbf{x}$ and it reflects the knowledge on $\mathbf{x}$ in monitoring design stage where the monitoring information has not been obtained; $f(z_{k,l}|\mathbf{x})$ is the likelihood function that quantifies influence of $\mathbf{x}$ on $Z_k$; and $f(z_{k,l}) = \int f(z_{k,l}|\mathbf{x})f(\mathbf{x})d\mathbf{x}$ is the normalizing constant independent of $\mathbf{x}$. The formulation of the likelihood function is pivotal to evaluating the $f(\mathbf{x}|z_{k,l})$ in Eq. (1). It necessitates a mathematical model (e.g., FEM and FDM) to link $\mathbf{x}$ to $Z_k$. For a given mathematical model, the POV (i.e., $z_{k,l}$) of $Z_k$ is modeled as:

$$z_{k,l} = M_k(\mathbf{x}) + \varepsilon_k \tag{2}$$

where $M_k(\mathbf{x})$ is the model prediction of the monitoring variable, referred as the monitoring performance function (MPF) of $Z_k$ in this study; $\varepsilon_k$ is assumed to be a Normal random variable with a mean value of $\mu_k$ and a standard deviation of $\sigma_k$, and it represents the model uncertainty associated with the mathematical model used to predict the value of $Z_k$. Using Eq. (2), the likelihood function $f(z_{k,l}|\mathbf{x})$ is given by:

$$f\left(z_{k,l}\,|\,\mathbf{x}\right)=\frac{1}{\sqrt{2\pi}\sigma_k}\exp\left\{-\frac{[z_{k,l}-M_k(\mathbf{x})-\mu_k]^2}{2\sigma_k^{\;2}}\right\} \tag{3}$$

Based on Eq. (3) and prior PDF of $\mathbf{x}$, $f(\mathbf{x}|z_{k,l})$, is obtained using Eq. (1). Then, $P_F\,(Z_k = z_{k,l})$ is calculated as:

$$P_F(Z_k=z_{k,l})=P(F|Z_k=z_{k,l})=\int I\left[g(\mathbf{x})\le 0\right]f(\mathbf{x}|z_{k,l})d\mathbf{x} \tag{4}$$

where $g(\mathbf{x})$ is the design performance function (DPF) of a geotechnical structure (e.g., $g(\mathbf{x})$ = $FS$-1) and it is used to assess whether the performance (e.g., slope stability) of the geotechnical structure is satisfactory or not; and $I[\cdot]$ is an indicator function. $I[\cdot]$ is equal to 1 if the performance of the geotechnical structure is unsatisfactory, i.e., $g(\mathbf{x}) \le 0$, otherwise, it is equal to zero.

Note that the model uncertainties associated with the MPF and DPF affect the posterior distribution of uncertain model parameters (see Eqs. (1)-(3)) and posterior reliability analysis (see Eq. (4)), future studies on which are warranted. This is, however, out of the scope of this study. The values of model uncertainties in the illustrative examples later are simply adopted from those used in the literature to enable a consistent comparison with previous studies.

The calculation of $P_F\,(Z_k = z_{k,l})$ involves a number of evaluations of the MPF (for Bayesian analysis) and DPF (for the reliability analysis), which requires mathematical models to predict the monitoring variable and design performance given $\mathbf{x}$. Consider, for example, using direct MCS or MCMCS to evaluate $f(\mathbf{x}|z_{k,l})$ in Eq. (1) and to calculate $P_F\,(Z_k = z_{k,l})$ in Eq. (4) by generating $N_{mcs}$ random samples of $\mathbf{x}$ (Beck and Au, 2002; Robert and Casella, 2004; Li et al., 2016c). This requires $N_{mcs}$ evaluations of MPF and DPF (i.e., $N_{mcs}$ evaluations of their corresponding mathematical models), respectively. A direct way to obtain the FPF with respect to $Z_k$ is repeatedly performing simulation runs at its $N_k$ POVs to calculate their corresponding $P_F(Z_k = z_{k,l})$ values. By this means, $N_{mcs} \times N_k$ evaluations of MPF and DPF are needed. This is often computationally expensive, particularly for complex numerical models (e.g., FEM and FDM). The next section proposes an efficient method for evaluating FPFwMV, which only requires a single run of direct MCS.

## 3 Reliability sensitivity analysis of monitoring variables using direct MCS and BUS

### *3.1 Bayesian updating with structural reliability methods (BUS)*

The proposed approach first evaluates the conditional PDF $f(\mathbf{x}|z_{k,l})$ given by Eq. (1) using a Bayesian updating technique recently developed by Straub and Papaioannou (2015), so-called Bayesian updating with structural reliability methods (BUS). BUS converts Bayesian updating problems into equivalent reliability analysis problems by constructing an observational failure domain (OFD) using the likelihood function. Reliability analysis methods (e.g., direct MCS) can then be used to evaluate the posterior distribution (e.g., Eq. (1)). In the context of BUS, the OFD in this study is defined as (Straub and Papaioannou, 2015; Cao et al., 2018):

$$\mathbf{\Omega}_{kl} = \left[ \mathrm{U} \le cf(z_{k,l} \,|\, \mathbf{x}) \right] \tag{5}$$

where $\mathbf{\Omega}_{kl}$ represents the OFD for $Z_k = z_{k,l}$; $c$ = a positive scalar constant ensuring $cf(z_{k,l}|\mathbf{x}) \le 1$ and it is taken as the reciprocal of the maximum value of the likelihood function $f(z_{k,l}|\mathbf{x})$ given by Eq. (3), i.e., $c = \sqrt{2\pi}\sigma_k$; and U = a uniform random variable ranging from zero to unity and it is independent of $\mathbf{x}$. Substituting Eq. (1) into Eq. (5) gives:

$$\mathbf{\Omega}_{kl} = \left[ \mathrm{U} \le \frac{f(\mathbf{x}|z_{k,l})}{\left[cf(z_{k,l})\right]^{-1} f(\mathbf{x})} \right] \tag{6}$$

where $[cf(z_{k,l})]^{-1}$ is a constant independent of $\mathbf{x}$. The $f(\mathbf{x}|z_{k,l})$ and $f(\mathbf{x})$ in Eq. (6) can be, respectively, viewed as the target and sampling distributions according to rejection sampling principle (Au and Wang, 2014; Straub and Papaioannou, 2015; Cao et al., 2018). It is reasoned that random samples of $\mathbf{x}$ generated from $f(\mathbf{x})$ and satisfying $\mathbf{\Omega}_{kl}$ follow $f(\mathbf{x}|z_{k,l})$. In other words, the $\mathbf{x}$ samples distributed as $f(\mathbf{x}|z_{k,l})$ can be obtained by simulating conditional samples from $f(\mathbf{x})$ satisfying $\mathbf{\Omega}_{kl}$ defined by Eq. (5). For example, a direct MCS run is performed to generate $N_{mcs}$ random samples of $\mathbf{x}$ from $f(\mathbf{x})$. The probability of each $\mathbf{x}$ sample falling into $\mathbf{\Omega}_{kl}$ is equal to $cf(z_{k,l}|\mathbf{x})$. The conditional samples of $\mathbf{x}$ satisfying $\mathbf{\Omega}_{kl}$ are selected from $N_{mcs}$ unconditional samples by simulating $N_{mcs}$ values, $\mathrm{U}_i$, $i$ = 1, 2, …, $N_{mcs}$, of U and comparing the $\mathrm{U}_i$ value with $cf(z_{k,l}|\mathbf{x})$ for the $i$-th sample. If $\mathrm{U}_i \le cf(z_{k,l}|\mathbf{x}_i)$, the sample falls into $\mathbf{\Omega}_{kl}$ and is accepted as the conditional sample of $\mathbf{x}$ given $Z_k = z_{k,l}$; otherwise, it is rejected. By this means, a number, $N_{a,l}$, of $\mathbf{x}$ samples distributed as $f(\mathbf{x}|z_{k,l})$ are obtained, where $N_{a,l} < N_{mcs}$, and these samples are used to evaluate the FPF with respect to $Z_k$.

### *3.2 Calculating FPFwMV using direct MCS and BUS*

The conditional samples (i.e., $\mathbf{x}_j$, $j$ = 1, 2, …, $N_{a,l}$) of $\mathbf{x}$ obtained from direct MCS and BUS represent $f(\mathbf{x}|z_{k,l})$ numerically, and they are used in Eq. (4) to evaluate $P_F(Z_k = z_{k,l})$:

$$P_F(Z_k = z_{k,l}) = \int I[g(\mathbf{x}) \le 0] f(\mathbf{x}|z_{k,l}) d\mathbf{x} = \frac{1}{N_{a,l}} \sum_{j=1}^{N_{a,l}} I[g(\mathbf{x}_j) \le 0] \tag{7}$$

A straightforward way to obtain FPF with respect to monitoring variable $Z_k$ is to perform repeated runs of direct MCS and BUS for the $N_k$ POVs (i.e., $z_{k,l}$, $l = 1, 2, \ldots, N_k$) of $Z_k$ to obtain their corresponding failure probabilities. By this means, $N_k$ direct MCS runs are needed, and the total computational efforts include $N_{mcs} \times N_k$ evaluations of the MPF in Bayesian analysis and $\sum_{l=1}^{N_k} N_{a,l}$ evaluations of the DPF, which remains a computationally expensive task.

Alternatively, this study proposes a sample-based strategy to select conditional samples of $\mathbf{x}$ given different POVs of $Z_k$ based on the same set of unconditional samples generated from $f(\mathbf{x})$ using direct MCS, by which the FPF with respect to $Z_k$ is evaluated by a single direct MCS run. Under the BUS framework, selection of the conditional samples of $\mathbf{x}$ from direct MCS samples depends on the likelihood function and the POV (i.e., $z_{k,l}$) of $Z_k$ (see Eq.(5)). As $z_{k,l}$ changes from $z_{k,1}$ to $z_{k,N_k}$, the likelihood function changes, so does $\boldsymbol{\Omega}_{kl}$. On the contrary, direct MCS samples simulated from $f(\mathbf{x})$ are independent of $z_{k,l}$. Based on these observations, the respective conditional samples of $\mathbf{x}$ given different POVs of $Z_k$ can be identified from the same set of direct MCS samples generated from $f(\mathbf{x})$ to calculate their corresponding failure probabilities without the need of performing repeated simulation runs for different POVs of $Z_k$. The implementation procedure is summarized in Fig. 2:

(1) Determine $N_k$ POVs (i.e., $z_{k,l}$, $l = 1, 2, \ldots, N_k$) of $Z_k$ for reliability sensitivity analysis;

(2) Generate $N_{mcs}$ samples (i.e., $\mathbf{x}_1, \mathbf{x}_2, \ldots, \mathbf{x}_{N_{mcs}}$) of $\mathbf{x}$ from $f(\mathbf{x})$ by direct MCS;

(3) Calculate respective values of the likelihood function $f(z_{k,l}\,|\mathbf{x})$ (see Eq. (3)) for $z_{k,l}$ given $\mathbf{x}_1, \mathbf{x}_2, \ldots, \mathbf{x}_{N_{mcs}}$, and their corresponding acceptance probabilities $cf(z_{k,l}|\mathbf{x})$ as conditional samples of $\mathbf{x}$ given $Z_k = z_{k,l}$;

(4) Generate $N_{mcs}$ random numbers (i.e., $U_1$, $U_2$, …, $U_{Nmcs}$) from a uniform distribution ranging from zero to unity, each of which corresponds to one **x** sample generated in step (2) and is used to determine whether the **x** sample satisfies Eq. (5) or not. This step selects $N_{a,l}$ conditional samples of **x** from $N_{mcs}$ unconditional samples generated in step (3);

(5) Evaluate $P_F\,(Z_k = z_{k,l})$ by Eq. (7) based on the $N_{a,l}$ conditional samples of **x** obtained in step (4);

(6) Repeat steps (3)-(5) $N_k$ times for $z_{k,l}$, $l$ = 1, 2, …, $N_k$, to obtain their corresponding values of $P_F\,(Z_k = z_{k,l})$.

The values of $P_F\,(Z_k = z_{k,l})$ obtained from the above procedure provide a discrete approximation of the FPF with respect to $Z_k$. During the calculation, direct MCS samples generated in step (2) remain unchanged. Hence, the MPF values (i.e., $M_k(\mathbf{x}_1)$, $M_k(\mathbf{x}_2)$, ..., $M_k(\mathbf{x}_{N_{mcs}})$) needed for evaluating the likelihood function in step (3) are the same for different POVs of $Z_k$. Only $N_{mcs}$ evaluations of MPF are needed in Bayesian analyses with different POVs of $Z_k$, leading to significant reduction in computational efforts. Specifically, $N_{mcs} \times (N_k - 1)$ evaluations of MPF are avoided in comparison with using repeated simulation runs. For different POVs, their corresponding OFDs (i.e., $\Omega_{kl}$, $l$ = 1, 2, …, $N_k$) may share some conditional samples because the OFDs of different POVs of $Z_k$ may intersect and their conditional samples are selected from the same set of direct MCS samples. As a result, using the sample-based strategy proposed in this study, the number of evaluations of DPF needed in reliability analyses (i.e., step (5)) is less than $\sum_{l=1}^{N_k} N_{a,l}$ . The computational effort for evaluating FPF with respect to $Z_k$ is further reduced.

In the above procedure, determining conditional samples for different POVs of $Z_k$ (see steps (2)-(4)) follows the original rejection sampling (ORS) principle (e.g., Au and Wang, 2014; Straub and Papaioannou, 2015), by which each unconditional sample of $\mathbf{x}$ has a probability of $cf(z_{k,l}|\mathbf{x})$ to be accepted as the conditional sample. The expected number $E(N_{a,l})$ of conditional samples given $Z_k = z_{k,l}$ is equal to $\sum_{i=1}^{N_{mcs}} cf(z_{k,l} \mid \mathbf{x}_i)$. However, due to random fluctuation in simulating $U_1, U_2, \ldots, U_{Nmcs}$ in step (4), the $N_{a,l}$ value determined from a given set of direct MCS samples can be either less or greater than $E(N_{a,l})$. This subsequently results in the fluctuation of estimated $P_F(Z_k = z_{k,l})$ in step (5) of the proposed sample-based strategy. More importantly, the number $N_{a,l}$ of conditional samples obtained in step (4) may not be sufficient to give an accurate estimate of $P_F(Z_k = z_{k,l})$ for different POVs. To address these issues, this paper proposes a modified rejection sampling (MRS) principle in the next section and combines the MRS principle with the sample-based strategy developed in this section to improve the accuracy of estimated $P_F(Z_k = z_{k,l})$.

## 4 Modified rejection sampling principle

As mentioned above, the unconditional sample generated by direct MCS is accepted or rejected as the conditional samples based on a probabilistic criterion (see Eq. (5)) according to the ORS principle. An unconditional sample $\mathbf{x}_i$ ($i$ = 1, 2, …, $N_{mcs}$) is accepted as the conditional sample if the random number $U_i$ is less than the acceptance probability $cf(z_{k,l}|\mathbf{x}_i)$ of $\mathbf{x}_i$; otherwise, it is rejected. In other words, for a given POV (e.g., $z_{k,l}$) of $Z_k$, the acceptance or rejection of $\mathbf{x}_i$ as the conditional sample depends on the random sample $U_i$ of U ranging zero and unity. Due to the randomness in U, the $\mathbf{x}_i$ may or may not be the conditional sample in different simulation runs that generate different U values, resulting in random fluctuation of conditional samples of $\mathbf{x}$ determined using ORS based on the same set of unconditional samples.

With the understanding of the random mechanism of determining conditional samples by ORS, the MRS principle is proposed in this study, which consists of a number, $N_r$, of ORS runs based on the same set of direct MCS samples (e.g., $\mathbf{x}_1$, $\mathbf{x}_2$, ..., $\mathbf{x}_{Nmcs}$) to reduce the random fluctuation of conditional samples. As for the sample-based strategy described in the preceding subsection, this means repeatedly performing step (4) $N_r$ times based on the same set of unconditional samples generated in step (2), as shown in Fig. 2 by dashed lines. Each run provides a set of conditional samples, which is denoted by $\mathbf{\Omega}_{kl,m}$, $m$ = 1, 2, …, $N_r$. According to the ORS principle, the conditional samples in $\mathbf{\Omega}_{kl,m}$ follow the target PDF, e.g., posterior PDF $f(\mathbf{x}|z_{k,l})$ of $\mathbf{x}$ under the BUS framework. Hence, the conditional samples in $\mathbf{\Omega} = [\mathbf{\Omega}_{kl,1}, \mathbf{\Omega}_{kl,2}, \ldots, \mathbf{\Omega}_{kl,Nr}]$ obtained in the $N_r$ runs of ORS (i.e., MRS) also follow the posterior PDF of $\mathbf{x}$. These conditional samples of $\mathbf{x}$ are subsequently used to evaluate $P_F\,(Z_k= z_{k,l})$ in step (5) of the proposed sample-based strategy and to obtain the FPF with respect to $Z_k$ in step (6).

Using the MRS principle, the unconditional samples (e.g., $\mathbf{x}_1$, $\mathbf{x}_2$, ..., $\mathbf{x}_{Nmcs}$) generated from $f(\mathbf{x})$ using direct MCS represent the $f(\mathbf{x})$ numerically and remain unchanged in different runs of ORS for determining conditional samples. Each unconditional sample $\mathbf{x}_i$ is considered $N_r$ times by generating $N_r$ samples of U, during which its acceptance probability $cf(z_{k,l}|\mathbf{x}_i)$ is fixed for a given $Z_k = z_{k,l}$, and the expected times of $\mathbf{x}_i$ to be accepted as conditional samples is equal to $cf(z_{k,l}|\mathbf{x}_i)\times N_r$. As $N_r$ increases, the frequency of $\mathbf{x}_i$ ($i$ = 1, 2, …, $N_{mcs}$) among conditional samples in $\mathbf{\Omega}$ obtained from the MRS principle converges to $cf(z_{k,l}|\mathbf{x}_i)\times N_r$, indicating that the random fluctuation in conditional samples of $\mathbf{x}$ obtained using MRS is minimal for large values of $N_r$. Correspondingly, the number of conditional samples in $\mathbf{\Omega}$ converges to $\sum_{i=1}^{N_{mcs}} cf(z_{k,l} \mid \mathbf{x}_i) N_r$, which increases with the increase of $N_r$. Both the increase in the number of conditional samples of $\mathbf{x}$ and the reduction in random fluctuation of the conditional samples contribute to improvement of the accuracy of estimated $P_F(Z_k = z_{k,l})$. Such an improvement is at the expense of ignorable additional computational costs in comparison of using ORS in the proposed sample-based strategy because the unconditional samples (e.g., $\mathbf{x}_1$, $\mathbf{x}_2$, ..., $\mathbf{x}_{N_{mcs}}$) and their corresponding likelihood functions $f(z_{k,l}|\mathbf{x}_i)$ for a given $Z_k = z_{k,l}$ are fixed in the $N_r$ runs of ORS.

Determinating $N_r$ is essential to the MRS principle. Since increasing $N_r$ leads to ignorable additional computational effort, a relatively large value (e.g., $N_r > 50$) of $N_r$ is suggested. On the other hand, as $N_r$ increases, the frequency of $\mathbf{x}_i$ ($i$ = 1, 2, …, $N_{mcs}$) among conditional samples in $\mathbf{\Omega}$ converge to $cf(z_{k,l}|\mathbf{x}_i)\times N_r$, leading to a stationary distribution of conditional samples of $\mathbf{x}$, and the convergence in estimated $P_F(Z_k = z_{k,l})$. In such case, it is not necessary to further increase $N_r$. This study suggests determining the $N_r$ adaptively based on the converge check of estimated $P_F(Z_k = z_{k,l})$, which is demonstrated using the illustrative example in the next section.

## 5. Illustration and validation of FPFwMV using a levee head monitoring example

With a complex numerical model (e.g., FDM and FEM), it is computationally prohibitive to validate the FPFwMV obtained from the proposed approach. To illustrate and validate the proposed approach for evaluating FPFwMV, this section uses a levee head monitoring example with explicit MPF and DPF. The next section illustrates the application of the proposed approach in the displacement monitoring design of a rock slope based on FDM.

The levee head monitoring example concerns about the occurrence of uplift on the downstream side of the levee shown in Fig. 3. The example was used to illustrate reliability updating with hydraulic head monitoring data under a Bayesian framework by Schweckendiek and Vrouwenvelder (2013) and Schweckendiek (2014). As shown in Fig. 3, there is an aquifer underlying the levee with a blanket layer on the downstream side with low permeability. The hydraulic head $\phi_{exit}$ at the potential exit location in the aquifer just under the lower blanket boundary is monitored in this example. The MPF is given by (Schweckendiek and Vrouwenvelder 2013):

$$\phi_{exit}=h_p+\lambda(h-h_p)+\varepsilon \tag{8}$$

where $h_p$ = phreatic surface in or above the blanket layer at the monitoring location, assumed to be equal to water level $h_s$ at the downstream surface; $h$ = upperstream water level, taken to be 3.9 m for a 100 year return period; λ = a damping factor for predicting the head difference in the aquifer at the potential exit point; $\varepsilon$ = a Normal variable with mean $\mu_\varepsilon$=0 and standard deviation $\sigma_\varepsilon$ =0.1 m, modeling the error between the monitoring value and model prediction of $\phi_{exit}$, which are adopted from those used by Schweckendiek and Vrouwenvelder (2013) to enable a consistent comparison. Uplift occurs as the hydraulic head difference $\Delta\phi$ between $\phi_{exit}$ and $h_p$ exceeds the hydraulic resistance that is represented by the critical uplift head difference $\Delta\phi_c'$. The uplift DPF is given by (Schweckendiek and Vrouwenvelder 2013):

$$g_{DPF}\left(\mathbf{x}\right)=\Delta\phi_c\,'-\Delta\phi \tag{9}$$

where $\Delta\phi$ and $\Delta\phi_c'$ are, respectively, calculated as:

$$\Delta\phi=\phi_{exit}-h_p=\lambda\left(h-h_p\right) \tag{10}$$

$$\Delta\phi_c\,'=m_u d\left(\gamma_{sat}/\gamma_w-1\right) \tag{11}$$

and $m_u$ = a model factor quantifying the uncertainty associated with the estimated critical uplift head difference; $d$ = the blanket layer thickness at the monitoring point; $\gamma_{sat}$ and $\gamma_w$ are the saturated volumetric weight of the blanket layer and the volumetric weight of water, respectively. Using Eqs. (9)-(11), the levee uplift reliability in this example depends on $h$, $h_p$, $d$, $m_u$, λ, and $\gamma_{sat}$. The distribution types and statistics of these uncertain parameters are summarized in Table 1. Assuming no correlation based on prior information, the prior distribution is the product of marginal distributions of uncertain model parameters (e.g., Cao et al., 2016).

### *5.1 Computation steps for evaluating FPF with respect to $\phi_{exit}$*

This section focuses on the validation of FPFwMV obtained from the proposed approach, where only one monitoring variable is considered, i.e., $Z$ = $\phi_{exit}$. To evaluate the FPF of $\phi_{exit}$, the six steps of the proposed approach described in Subsection 3.2 are implemented as follows:

(1) For determining the POVs of $\phi_{exit}$, the statistical information of uncertain model parameters summarized in Table 1 is used to generate 1,000,000 unconditional samples of uncertain model parameters by direct MCS. These samples are used to predict $\phi_{exit}$, yielding 1,000,000 estimates of $\phi_{exit}$. Using these estimates, the mean value $\mu_\phi$ and standard deviation

$\sigma_\phi$ of $\phi_{exit}$ are calculated as 3.18 m and 0.36 m, respectively. A series of POVs of $\phi_{exit}$ ranging from $\mu_\phi - 3\times\sigma_\phi$ (i.e., 2.1 m) to 3.9 m are considered, as shown in Table 2. The lower bound (i.e., 2.1 m) of the range of $\phi_{exit}$ is determined as its lowest conceivable value based on the three-sigma rule (e.g., Duncan, 2000), and its upper bound is considered not exceeding a 100-year upperstream water level $h$=3.9 m in this example. Correspondingly, the normalized POVs $(\phi_{exit}-\mu_\phi)/\sigma_\phi$ of $\phi_{exit}$ in this example vary from –3.0 to 2.0 with an increment of 0.5, which are summarized in Table 2. Note that although the POVs of $\phi_{exit}$ are determined through direct MCS in this example, this is not necessary for implementing the proposed approach because POVs of monitoring variables can also be determined or selected by engineering experience and judgments;

(2) If direct MCS is performed to determine POVs of $\phi_{exit}$ in step (1), the 1,000,000 unconditional samples generated in step (1) are used in this step; otherwise, a direct MCS run is performed to generate unconditional samples from the prior distribution;

(3) For each POV of $\phi_{exit}$ shown in Table 2, the respective values of likelihood function for different unconditional samples of uncertain model parameters generated in step (1) or (2) are calculated by:

$$f\left(\phi_{exit} \mid \mathbf{x}\right) = \frac{1}{\sqrt{2\pi}\sigma_\varepsilon} \exp\left\{ -\frac{[\phi_{exit} - h_p - \lambda(h - h_p)]^2}{2\sigma_\varepsilon{}^2} \right\} \tag{12}$$

and the acceptance probability of unconditional samples is calculated as $cf(\phi_{exit}|\mathbf{x})$, where $c$ is taken as equal to $\sqrt{2\pi}\sigma_\varepsilon \approx 0.25$ in this example;

(4) Generate 1,000,000 random numbers uniformly distributed from zero to unity, each of which corresponds to one unconditional sample generated in previous steps and is used to

determine whether the sample is accepted as a conditional sample according to its acceptance probability calculated in step (3);

(5) By the MRS principle, step (4) is repeatedly performed $N_r$ times to reduce the random fluctuation in selected conditional samples, which are subsequently used to evaluate the conditional uplift failure probability given a POV of $\phi_{exit}$. Here, the $N_r$ is gradually increased until the estimated uplift failure probability converges. For example, Fig. 4 shows the variation of the uplift failure probability $P_F\,(\phi_{exit}$=2.1 m) given $\phi_{exit}$ = 2.1 m with the increase of $N_r$. As $N_r$ increases from 1 to 20, the estimated $P_F\,(\phi_{exit}$=2.1 m) value gradually converges to 0.0020. A relatively large value (i.e., 100) of $N_r$ is adopted in the MRS principle to ensure the convergence of the uplift failure probability;

(6) Repeat steps (3)-(5) for each POV of $\phi_{exit}$ shown in Table 2 to obtain their corresponding conditional uplift failure probabilities, which provide a discrete approximation of the FPF with respect to $\phi_{exit}$.

### *5.2 FPF with respect to the hydraulic head at the monitoring location*

Fig. 5 shows the FPF with respect to $\phi_{exit}$ obtained from the proposed approach by a line with circles. As the normalized POVs of $\phi_{exit}$ increases from −3 to 2 (i.e., $\phi_{exit}$ increases from 2.1 to 3.9 m), the uplift failure probability increases by two orders of magnitude from 0.0020 to 0.19. Monitoring the hydraulic head effectively senses the variation of the occurrence plausibility of uplift. Moreover, the FPF with respect to $\phi_{exit}$ provides an overview of the variation of the uplift reliability as a function of $\phi_{exit}$ prior to monitoring instrumentation. Based on the FPF with respect to $\phi_{exit}$, the uplift failure probability can be determined directly from the observational value of $\phi_{exit}$ during monitoring, which facilitates real-time risk-based decision making. For example, as the observational value of $\phi_{exit}$ is equal to 2.3 m, the corresponding uplift failure probability reads as around 0.0042 from the FPF shown in Fig. 5, which is consistent with the value (0.0048) reported by Schweckendiek and Vrouwenvelder (2013).

### *5.3 Results comparison*

For further validation, the uplift failure probabilities given different POVs are also calculated using a total of 11 runs of MCMCS. In each run, 1,000,000 MCMCS samples are generated to numerically represent the posterior distribution given by Eq. (1) and to evaluate the uplift failure probability given by Eq. (4) for a POV of $\phi_{exit}$. Fig. 5 also includes the FPF with respect to $\phi_{exit}$ obtained from repeated MCMCS runs by a line with squares. The lines with circles and squares are close to each other. This indicates that the two sets of results obtained from the proposed approach and repeated MCMCS runs are in a good agreement. This validates the proposed approach. It is should be noted that only one direct MCS run is used to evaluate the FPF with respect to $\phi_{exit}$ by the proposed approach, avoiding performing repeated simulation runs for different POVs of $\phi_{exit}$.

For a given POV of $\phi_{exit}$, using the MRS principle in the proposed approach needs to re-run $N_r$ (e.g., 100) times of ORS for selection of conditional samples of uncertain model parameters based on the same set of unconditional samples. The computational effort needed in the proposed approach with MRS is, however, comparable with those needed for using the proposed approach with ORS (i.e., $N_r = 1$) because the additional computational effort needed for re-running ORS based on the same set of unconditional samples is negligible. For comparison, Fig. 5 shows the FPF with respect to $\phi_{exit}$ obtained from the proposed approach with ORS by a line with triangles. When the uplift failure probability is greater than 0.01, the FPF obtained from the proposed approach with ORS agrees well with that obtained from the proposed approach with MRS and repeated MCMCS runs. The agreement deteriorates as the uplift failure probability is less than 0.01. The FPF obtained using ORS is not accurate at low failure probability levels, while using the MRS in the proposed approach provides consistent results.

Fig. 6 compares the coefficient of variation (COV) of the uplift failure probability at the same POV of $\phi_{exit}$ obtained from the proposed approach with ORS and MRS (see triangles and circles, respectively). The COV value at a given POV of $\phi_{exit}$ in Fig. 6 is calculated from 100 estimates of the uplift failure probability at the POV obtained from 100 runs of the proposed approach with ORS or MRS. As shown in Fig. 6, for a given POV of $\phi_{exit}$, the triangle always appears above the circle. Using the MRS principle in the proposed approach leads to reduction in COV of the estimated uplift failure probability. These observations demonstrate the benefit of using the MRS principle in the proposed approach, particularly in relatively low failure probability regime.

## 6. Reliability sensitivity analysis for rock slope displacement monitoring using FDM

The proposed approach with MRS is next applied to analyzing the reliability sensitivity on surface displacements monitored at different locations of a rock slope example (Li et al., 2016c). As shown in Fig. 7, the rock slope has a height of 12 m and a slope angle of 60°. There is a joint extending from the slope toe to the height of 7.65 m in a direction at an angle of 35° to the horizontal. It intersects a vertical tension crack that locates behind the slope crest at a distance of 4 m and has a depth of 4.35 m. The groundwater condition is also shown in Fig. 7, and is characterized by the ratio $r_w$ of water depth $D_w$ over the crack depth $D_c$, i.e., $r_w = D_w / D_c$, which is represented by a truncated exponential variable ranging from 0 to 1 and having a mean of 0.1 (Li et al., 2016c). In addition to $r_w$, the cohesion $c_J$, friction angle $\phi_J$, and Young's modulus $E$ of the joint and the surcharge load $p$ are represented by Normal random variables. Their statistics are summarized in Table 3, which are consistent with those adopted by Li et al. (2016c). In addition, as shown in Fig. 7, the slope is reinforced by four rows of rock bolts. For the sake of conciseness, more details on the rock bolts and the properties of rock masses are referred to Li et al. (2016c).

The $FS$ of rock slope stability and the surface displacements are evaluated using FDM through a commercial software FLAC 7.0 (Itasca, 2014). Fig. 8 shows dimensions of the FDM that is discretized into 782 elements. The rock mass and the joint are modeled as elastic-perfectly plastic materials based on the Mohr-Coulomb strength criterion, and the rock bolts are modeled through cable elements. The bottom boundary is fixed in both horizontal and vertical directions and the right vertical boundary is constrained in horizontal direction. Moreover, the groundwater condition is considered through a groundwater table. The set-up of the FDM in this study is generally consistent with that adopted by Li et al. (2016c), which provides more details on development of the FDM of the rock slope for interested readers.

For validation, the $FS$ and surface displacements at two different points (i.e., A and B shown in Fig. 7) are calculated using the FDM developed in this study under different surcharge loads and groundwater levels, and the results are compared with those (including $FS$, vertical displacement ($V_A$) at point A, and horizontal displacement ($H_B$) at point B) reported by Li et al. (2016c). Fig. 9(a) shows the $FS$, $V_A$, and $H_B$ calculated under different surcharge loads in this study and Li et al. (2016c) by solid and dashed lines, respectively. The results obtained from this study are consistent with those reported by Li et al. (2016c). Similar observations can also be obtained from the $FS$, $V_A$, and $H_B$ calculated under different groundwater levels, as shown in Fig. 9 (b). This validates the FDM developed in this study. The FDM is subsequently used in the proposed approach to evaluate FPF with respect to surface displacements for reliability sensitivity analysis. This is different from Li et al. (2016c), where surrogate models (i.e., second-order polynomial response surfaces) are used to back analyze model parameters (e.g., $r_w$, $c_J$, $\phi_J$, $E$, and $p$) for assessing slope stability safety and reliability based on monitoring information under a Bayesian framework. The surrogate model is adopted to reduce computational efforts needed in the back analysis, safety assessment, and reliability analysis so that repeated simulation runs for different values of monitoring variables are tractable. However, it shall be noted that the accuracy of surrogate model is problem-dependent. Future studies on surrogate model-based Bayesian analyses, where the probability space of uncertain parameters is updated with acquired information, are warranted, which is out of scope of this study. Alternatively, this study tackles the computational difficulty arising from sophisticated numerical models in evaluating FPFwMV through developing an efficient reliability sensitivity analysis method, where repeated simulation runs are avoided, as illustrated below.

### *6.1 Computation steps for evaluating FPFwMV in the rock slope example*

For the purpose of reliability sensitivity analysis of monitoring variables, two additional monitoring locations (i.e., points C and D shown in Fig. 7) are considered besides points A and B in this study, whose horizontal and vertical displacements are also taken as monitoring variables. As a result, there are a total of eight monitoring variables $Z_k$, $k$ = 1, 2, …, 8 (i.e., horizontal displacements $H_A$, $H_B$, $H_C$, and $H_D$, and vertical displacements $V_A$, $V_B$, $V_C$ and $V_D$), of points A to D. Then, the proposed approach with the MRS principle is applied to evaluating the FPF of each monitoring variable concerned (i.e., $H_A$, $H_B$, $H_C$, $H_D$, $V_A$, $V_B$, $V_C$ and $V_D$), which is described as follows:

(1) The implementation starts with prescribing POVs of monitoring variables. In this example, 13 POVs varying from 1 to 13mm at an interval of 1mm are considered for each monitoring variable;

(2) A direct MCS with 15,000 samples is simulated from the prior distribution of uncertain model parameters (i.e., $r_w$, $c_J$, $\phi_J$, $E$, and $p$). Herein, assuming no correlation among uncertain model parameters based on prior information, the prior distribution is the product of their marginal distributions summarized in Table 3. Using 15,000 samples to evaluate the failure probability of the rock slope stability based on the prior distribution and FDM, where the model error in $FS$ calculated by FDM is considered as a Normal distribution with a mean of 0 and standard deviation of 0.05 (Li et al. 2016c). The resulting failure probability is 25.5%,

which agrees well with the value (i.e., 24.9%) reported by Li et al. (2016c). This further validates the uncertainty model and FDM developed in this study;

(3) For a given POV of the monitoring variable concerned, the values of the likelihood function for the 15,000 unconditional samples are calculated using Eq. (3), where the MPF is calculated using the FDM, and the acceptance probability of a given sample is evaluated as the product of the constant $\sqrt{2\pi}\sigma_k$ and the likelihood function for the sample. In this example, the prediction model error $\varepsilon_k$ in surface displacements is represented by a Normal random variable with a mean of 0 and standard deviation (i.e., $\sigma_k$) of 1 mm, which follow those adopted by Li et al. (2016c);

(4) Generate 15,000 random numbers uniformly distributed from zero to unity, each of which corresponds to one unconditional sample for selecting conditional samples;

(5) Step (4) is repeatedly performed 100 times (i.e., $N_r$ = 100) to reduce the random fluctuation in conditional samples, which are subsequently used to evaluate the conditional failure probability of the rock slope stability given the POV of the monitoring variable concerned by Eq. (7);

(6) Repeat steps (3)-(5) for each POV of the monitoring variable concerned to obtain their corresponding conditional failure probabilities of the rock slope stability, which provide a discrete approximation of the FPF of the monitoring variable.

### *6.2 FPFs with respect to surface displacements*

Fig. 10 shows the FPFs with respect to horizontal displacements (i.e., $H_A$, $H_B$, $H_C$, and $H_D$) and vertical displacements (i.e., $V_A$, $V_B$, $V_C$, and $V_D$) by solid and dashed lines, respectively. As the surface displacement increases, the slope failure probability increases by two to three orders of magnitude. This means that the reliability level of the rock slope stability is generally sensitive to surface displacements, particularly as the surface displacement is relatively small (say less than 7 mm in this example). It is also observed that the reliability sensitivity of the rock slope stability depends on the monitoring location because different FPFs are obtained for surface displacements at different locations. Comparing FPFs with respect to the eight monitoring variables reveals that the horizontal displacement $H_B$ at point B (i.e., the slope toe) is the most sensitive monitoring variable while its vertical displacement $V_B$ is the least sensitive one. It shall be emphasized that calculations of the FPFs of the eight monitoring variables are based on the same set of unconditional samples using the proposed approach. This avoids repeatedly performing direct MCS runs for different monitoring variables and for different POVs of a given monitoring variable in this example. The number of evaluations of numerical models needed for evaluating the FPFs is reduced considerably, leading to significant computational saving.

### *6.3 Reliability sensitivity to surface displacements at different locations*

For detailed examination of the reliability sensitivity on different monitoring variables, a reliability sensitivity index (RSI) is defined in this example, and it is written as:

$$RSI_k = \frac{\ln P_F(Z_k = POV_{k,\max}) - \ln P_F(Z_k = POV_{k,\min})}{POV_{k,\max} - POV_{k,\min}} \tag{13}$$

where $Z_k$, $k$ = 1, 2, …, 8, are the eight monitoring variables; $POV_{k,\min}$ and $POV_{k,\max}$ are the minimum and maximum POVs of $Z_k$, and they are, respectively, taken as 1 mm and 13 mm in this example; $\ln P_F(Z_k = POV_{k,\min})$ and $\ln P_F(Z_k = POV_{k,\max})$ are logarithms of the conditional failure probability of the rock slope stability given $Z_k = POV_{k,\min}$ and $POV_{k,\max}$, respectively. The $\mathrm{RSI}_k$ represents the increasing rate of the rock slope failure probability as the surface displacement increases from $POV_{k,\min}$ to $POV_{k,\max}$, and reflects the reliability sensitivity of the rock slope stability with respect to $Z_k$ ranging from $POV_{k,\min}$ to $POV_{k,\max}$. It provides a measure to, quantitatively, compare the reliability sensitivity on different monitoring variables. The greater the $\mathrm{RSI}_k$ is, the more sensitive to the reliability of the rock slope stability is. Table 4 summarizes the $\mathrm{RSI}_k$ values of the eight monitoring variables. The $H_B$ has the maximum RSI value (i.e., 0.58) among the eight monitoring variables while $V_B$ has the minimum RSI value (i.e., 0.36), which indicates that $H_B$ and $V_B$ are the most and least sensitive monitoring variables, respectively. This is consistent with the observation obtained from the FPFs shown in Fig. 10. Moreover, as shown in Table 4, the reliability sensitivity of the rock slope stability to horizontal displacements (i.e., $H_A$, $H_C$, $H_D$, and $H_B$) increases with the decrease of the elevation from point A to point B. In contrast, the reliability sensitivity of the rock slope stability to vertical displacements (i.e., $V_A$, $V_C$, $V_D$, and $V_B$) decreases with the decrease of the elevation from point A to point B. This suggests that the instrumentation shall be installed to monitor the horizontal displacement (i.e., $H_B$) at slope toe and the vertical displacement (i.e., $V_A$) at the top of tension crack with the first priority.

## 7 Summary and conclusions

This paper proposed a reliability sensitivity analysis method that leverages on the robustness of direct Monte Carlo simulation (MCS) and the recently established analogy between reliability and Bayesian updating problem, i.e., the BUS (Bayesian Updating with Structural Reliability Methods) framework. It allows one to use a single run of direct MCS to obtain failure probability functions (FPF) with respect to different monitoring variables (FPFwMV) for determining the most sensitive monitoring variables during monitoring design, where no monitoring information is available. To reduce the random fluctuation of conditional samples obtained from BUS, this study proposed a modified rejection sampling (MRS) principle that consists of multiple runs of the original rejection sampling (ORS) based on the same set of direct MCS samples.

The proposed approach has been illustrated and validated using a levee head monitoring example with a single monitoring variable and explicit performance functions and a rock slope example with multiple monitoring variables and implicit performance functions evaluated through the finite difference model (FDM). Results showed that the proposed approach efficiently generates the FPFwMV for monitoring design in the sense that it only needs a single run of direct MCS and avoids repeated simulation runs for evaluating failure probability at different possible observational values of a given monitoring variable. This leads to significant reduction in computation efforts for reliability sensitivity analysis of monitoring variables, particularly when sophisticated numerical models (e.g., FDM) is involved. Using the MRS principle improves the accuracy of FPFs at the expense of ignorable additional computational efforts in comparison with using ORS. In the rock slope example, the reliability sensitivity of slope stability to vertical and horizontal surface displacements has opposite trends. As the elevation of the monitoring location increases, the sensitivity to the horizontal displacement decreases, but the sensitivity to the vertical displacement increases. As a result, the horizontal displacement at the slope toe and the vertical displacement at the top of slope are the most critical monitoring variables, where monitoring instruments shall be installed with the first priority.

With the FPFwMV obtained prior to monitoring, in-situ instrumentation can be arranged in a cost-effective manner, and determining the real-time reliability level of geotechnical structures during monitoring is a trivial task. This is of great significance to practical monitoring problems in real word, where complex numerical models are often involved for detailed and realistic modeling of geotechnical structures concerned.

**Acknowledgements**

This work was supported by the National Key R&D Program of China (Project No. 2016YFC0800200), and the National Natural Science Foundation of China (Project Nos. 51579190, 51528901, 51679174). The second author would like to thank for the support of China Scholarship Council (No. 201606270085). The authors also would like to thank Dr. Xueyou Li for his advices on the calculation model of the rock slope example.

**Reference**

[1] Ang, A.H.S., Tang, W.H. (2007). Probability Concepts in Engineering: Emphasis on Applications to Civil and Environmental Engineering, seconded. John Wiley & Sons.

[2] Au, S.K. (2005). Reliability-based design sensitivity by efficient simulation. Computers and structures, 83(14):1048-61.

[3] Au, S.K., Wang, Y. (2014). Engineering risk assessment with subset simulation. John Wiley & Sons.

[4] Beck, J.L., Au, S.K. (2002). Bayesian updating of structural models and reliability using Markov chain Monte Carlo simulation. Journal of engineering mechanics, 128(4): 380-391.

[5] Cao, Z.J., Wang, Y. (2014). Bayesian model comparison and characterization of undrained shear strength. Journal of Geotechnical and Geoenvironmental Engineering, 140(6): 04014018.

[6] Cao, Z.J., Wang, Y., Li, D.Q. (2016). Quantification of prior knowledge in geotechnical site characterization. Engineering Geology, 203: 107-116.

[7] Cao, Z.J., Zheng, S., Li, D.Q., Phoon, K.K. (2018). Bayesian identification of soil stratigraphy based on soil behaviour type index. Canadian Geotechnical Journal, doi.org/10.1139/cgj-2017-0714.

[8] Camós, C., Špačková, O., Straub, D., Molins, C. (2016). Probabilistic approach to assessing and monitoring settlements caused by tunneling. Tunnelling and Underground Space Technology, 51: 313-325.

[9] Ching, J., Hsieh, Y.H. (2007). Local estimation of failure probability function and its confidence interval with maximum entropy principle. Probabilistic Engineering Mechanics, 22(1): 39-49.

[10] Duncan, J.M. (2000). Factors of safety and reliability in geotechnical engineering. Journal of geotechnical and geoenvironmental engineering, 126(4): 307-316.

[11] Ering, P., Babu, G.L.S. (2016). Probabilistic back analysis of rainfall induced landslide— a case study of Malin landslide, India. Engineering Geology, 208: 154-164.

[12] Gong, W., Juang, C.H., and Martin, J.R. (2017). A new framework for probabilistic analysis of the performance of a supported excavation in clay considering spatial variability. Géotechnique, 67(6): 546-552.

[13] Gong, W., Juang, C.H., Ii, J.R.M., Tang, H., Wang, Q., Huang, H. (2018). Probabilistic analysis of tunnel longitudinal performance based upon conditional random field simulation of soil properties. Tunnelling and Underground Space Technology, 73: 1-14.

[14] Hong, Y., Wang, L.Z., Ng, C. W.W., Yang, B. (2017). Effect of initial pore pressure on undrained shear behaviour of fine-grained gassy soil. Canadian Geotechnical Journal, 54(11): 1592-1600.

[15] Hsiao, E.C., Schuster, M., Juang, C.H., Kung, G.T. (2008). Reliability analysis and updating of excavation-induced ground settlement for building serviceability assessment. Journal of Geotechnical and Geoenvironmental Engineering, 134(10): 1448-1458.

[16] Itasca Consulting Group, Inc. 2014. https://www.itascacg.com/.

[17] Jiang, S.H., Papaioannou, I., Straub, D. (2018). Bayesian updating of slope reliability in spatially variable soils with in-situ measurements. Engineering Geology, 239: 310-320.

[18] Juang, C.H., Luo, Z., Atamturktur, S., Huang, H. (2013). Bayesian updating of soil parameters for braced excavations using field observations. Journal of Geotechnical and Geoenvironmental Engineering, 139(3): 395-406.

[19] Kyowa (2017). http://www.kyowa-ei.com/eng/product/sector/building/application_080.htm.

[20] Kelly, R., Huang, J. (2015). Bayesian updating for one-dimensional consolidation measurements. Canadian Geotechnical Journal, 52(9): 1318-1330.

[21] Li, D.Q., Zhang, F.P., Cao, Z.J., Zhou, W., Phoon, K.K., Zhou, C.B. (2015). Efficient reliability updating of slope stability by reweighting failure samples generated by Monte Carlo simulation. Computers and Geotechnics, 69: 588-600.

[22] Li, D.Q., Xiao, T., Cao, Z.J., Zhou, C.B., Zhang, L.M. (2016a). Enhancement of random finite element method in reliability analysis and risk assessment of soil slopes using Subset Simulation. Landslides, 13(2): 293-303.

[23] Li, S., Zhao, H., Ru, Z., Sun, Q. (2016b). Probabilistic back analysis based on Bayesian and multi-output support vector machine for a high cut rock slope. Engineering Geology, 203: 178-190.

[24] Li, X.Y., Zhang, L.M., Jiang, S.H., Li, D.Q., Zhou, C.B. (2016c). Assessment of slope stability in the monitoring parameter space. Journal of Geotechnical and Geoenvironmental Engineering, 142(7): 04016029.

[25] Li, X.Y., Zhang, L.M., Jiang, S.H. (2016d). Updating performance of high rock slopes by combining incremental time-series monitoring data and three-dimensional numerical analysis. International Journal of Rock Mechanics and Mining Sciences, 83: 252-261.

[26] Papaioannou, I., Straub, D. (2012). Reliability updating in geotechnical engineering including spatial variability of soil. Computers and Geotechnics, 42: 44-51.

[27] Peng, M., Li, X.Y., Li, D.Q., Jiang, S.H., Zhang, L.M. (2014) Slope safety evaluation by integrating multi-source monitoring information. Structural safety, 49: 65-74.

[28] Qi, X.H. and Li, D.Q. (2018). Effect of spatial variability of shear strength parameters on critical slip surfaces of slope. Engineering Geology, 239: 41-49.

[29] Schweckendiek, T., Vrouwenvelder, A. (2013). Reliability updating and decision analysis for head monitoring of levees. Georisk: Assessment and Management of Risk for Engineered Systems and Geohazards, 7(2): 110-121.

[30] Schweckendiek, T. (2014). On reducing piping uncertainties: A Bayesian decision approach. TU Delft, Delft University of Technology.

[31] Sudret, B. (2008). Global sensitivity analysis using polynomial chaos expansions. Reliability Engineering and System Safety, 93(7): 964-979.

[32] Straub, D. (2011). Reliability updating with equality information. Probabilistic Engineering Mechanics, 26(2): 254-258.

[33] Straub, D., Papaioannou, I. (2015) Bayesian updating with structural reliability methods. Journal of Engineering Mechanics, 141(3): 04014134.

[34] Wang, L., Ravichandran, N., Juang, C. H. (2012). Bayesian updating of KJHH model for prediction of maximum ground settlement in braced excavations using centrifuge data. Computers and Geotechnics, 44: 1-8.

[35] Wang, Y., Cao, Z.J., Au, S.K. (2010). Efficient Monte Carlo simulation of parameter sensitivity in probabilistic slope stability analysis. Computers and Geotechnics, 37(7-8): 1015-1022.

[36] Wang, Y. (2012). Uncertain parameter sensitivity in Monte Carlo simulation by sample reassembling. Computers and Geotechnics, 46: 39-47.

[37] Wang, Y., Cao, Z.J. (2013). Probabilistic characterization of Young's modulus of soil using equivalent samples. Engineering Geology, 159: 106-118.

[38] Xiao, T., Li, D.Q., Cao, Z.J., Au, S.K., Phoon, K.K. (2016). Three-dimensional slope reliability and risk assessment using auxiliary random finite element method. Computers and Geotechnics, 79: 146-158.

[39] Xiao, T., Li, D.Q., Cao, Z.J., Zhang, L.M. (2018). CPT-based probabilistic characterization of three-dimensional spatial variability using MLE. Journal of Geotechnical and Geoenvironmental Engineering, 144(5): 04018023

[40] Xu, L., Coop, M. C., Zhang, M. S., Wang, G. L. (2018). The mechanics of a saturated silty loess and implications for landslides. Engineering Geology, 236: 29-42.

[41] Yu, Y., Wang, E., Zhong, J., Liu, X., Li, P., Shi, M., Zhang, Z. (2014). Stability analysis of abutment slopes based on long-term monitoring and numerical simulation. Engineering Geology, 183: 159-169.

[42] Yuan, X. (2013). Local estimation of failure probability function by weighted approach. Probabilistic Engineering Mechanics, 34: 1-11.

[43] Zhang, J., Huang, H.W., Zhang, L.M., Zhu, H.H., Shi, B. (2014). Probabilistic prediction of rainfall-induced slope failure using a mechanics-based model. Engineering Geology, 168(1): 129-140.

[44] Zhang, J., Tang, W.H., Zhang, L.M., Huang, H.W. (2012). Characterising geotechnical model uncertainty by hybrid Markov Chain Monte Carlo simulation. Computers and Geotechnics, 43: 26-36.

[45] Zhang, J., Wang, H., Huang, H.W., Chen, L.H. (2017). System reliability analysis of soil slopes stabilized with piles. Engineering Geology, 229(7): 45-52.

[46] Zhang, L.L., Zhang, J., Zhang, L.M., Tang, W.H. (2010). Back analysis of slope failure with Markov chain Monte Carlo simulation. Computers and Geotechnics, 37(7): 905-912.

[47] Zhang, L.L., Zuo, Z.B., Ye, G.L., Jeng, D.S., Wang, J.H. (2013). Probabilistic parameter estimation and predictive uncertainty based on field measurements for unsaturated soil slope. Computers and Geotechnics, 48: 72-81.

[48] Zhang, W.G., Goh, A.T.C., Xuan, F. (2015). A simple prediction model for wall deflection caused by braced excavation in clays. Computers and Geotechnics, 63: 67-72.

[49] Zheng, D., Huang, J., Li, D.Q., Kelly, R., Sloan, S.W. (2018). Embankment prediction using testing data and monitored behaviour: A Bayesian updating approach. Computers and Geotechnics, 93: 150-162.

**Captions of Tables**

**Table 1.** Summary of distribution types and statistics of uncertain model parameters in the levee monitoring example (after Schweckendiek and Vrouwenvelder 2013)

**Table 2.** Summary of possible observational values of the hydraulic head in the aquifer

**Table 3.** Prior distribution of uncertain model parameters of the rock slope example (after Li et al. 2016c)

**Table 4.** Reliability sensitivity index of different monitoring variables

**Table 1. Summary of distribution types and statistics of uncertain model parameters in the levee monitoring example (after Schweckendiek and Vrouwenvelder 2013)**

| Model parameters | Distribution type | Statistical parameters | |
|---|---|---|---|
| | | Mean | Standard deviation |
| Water lever $h$ (m) | Gumbel | 2.67 | 0.38 |
| Surface level at the potential exit point $h_p$ (m) | Normal | 0.3 | 0.1 |
| Blanket layer thickness $d$ (m) | Lognormal | 3.0 | 0.5 |
| Model factor $m_u$ | Lognormal | 1.0 | 0.1 |
| Saturated volumetric weight of the blanket layer $\gamma_{\mathrm{sat}}$ (kN/m$^3$) | Normal | 20.0 | 1.0 |
| Damping factor $\lambda$ | Lognormal | 0.8 | 0.1 |

**Table 2. Summary of possible observational values of the hydraulic head in the aquifer**

| Possible observational value$\phi_{exit}$ ($m$) | 2.10 | 2.28 | 2.46 | 2.64 | 2.82 | 3.00 | 3.18 | 3.36 | 3.54 | 3.72 | 3.90 |
|---|---|---|---|---|---|---|---|---|---|---|---|
| Normalized value ($\phi_{exit}-\mu_\phi$)/$\sigma_\phi$ | -3.0 | -2.5 | -2.0 | -1.5 | -1.0 | -0.5 | 0 | 0.5 | 1.0 | 1.5 | 2.0 |

**Table 3. Prior distribution of uncertain model parameters of the rock slope example (after Li et al. 2016c)**

| Parameter | Distribution type | Mean value | Coefficient of variation |
|---|---|---|---|
| Young's modulus $E$ (MPa) | Normal | 50 | 0.2 |
| Cohesion $c_J$ (kPa) | Normal | 20 | 0.3 |
| Friction angle $\phi_J$ ($^{\circ}$) | Normal | 32 | 0.2 |
| Surcharge load $p$ (kPa) | Normal | 200 | 0.1 |
| Groundwater level ratio $r_w$ | Truncated exponential | 0.1 | 1 |

**Table 4. Reliability sensitivity index of different monitoring variables**

| Monitoring location | Monitoring variable | $RSI_k$ | Rank |
|---|---|---|---|
| 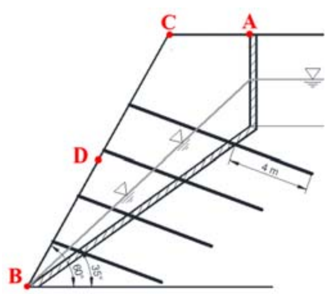  | $Z_1$: $H_A$ | 0.40 | 7 |
| | $Z_2$: $H_B$ | 0.58 | 1 |
| | $Z_3$: $H_C$ | 0.42 | 6 |
| | $Z_4$: $H_D$ | 0.51 | 3 |
| | $Z_5$: $V_A$ | 0.55 | 2 |
| | $Z_6$: $V_B$ | 0.36 | 8 |
| | $Z_7$: $V_C$ | 0.47 | 4 |
| | $Z_8$: $V_D$ | 0.43 | 5 |

**Captions of Figures**

**Fig. 1.** Reliability sensitivity analysis framework for monitoring variables

**Fig. 2.** Implementation procedure of the proposed sample-based strategy for evaluating FPFwMV

**Fig. 3.** The levee head monitoring example (after Schweckendiek and Vrouwenvelder 2013)

**Fig. 4.** Variation of the uplift failure probability given $\phi_{exit}$ = 2.1 m with the increase of $N_r$

**Fig. 5.** Comparison of uplift failure probability functions obtained by different methods

**Fig. 6.** Coefficients of variation of uplift failure probabilities calculated by the proposed approach with ORS and MRS

**Fig. 7.** Illustration of the rock slope example (after Li et al. 2016)

**Fig. 8.** The finite difference model for the rock slope example in FLAC 7.0

**Fig. 9.** Factor of safety and surface displacements at points A and B under different surcharge load and groundwater levels

**Fig. 10.** Failure probability functions with respect to different monitoring variables in the rock slope example

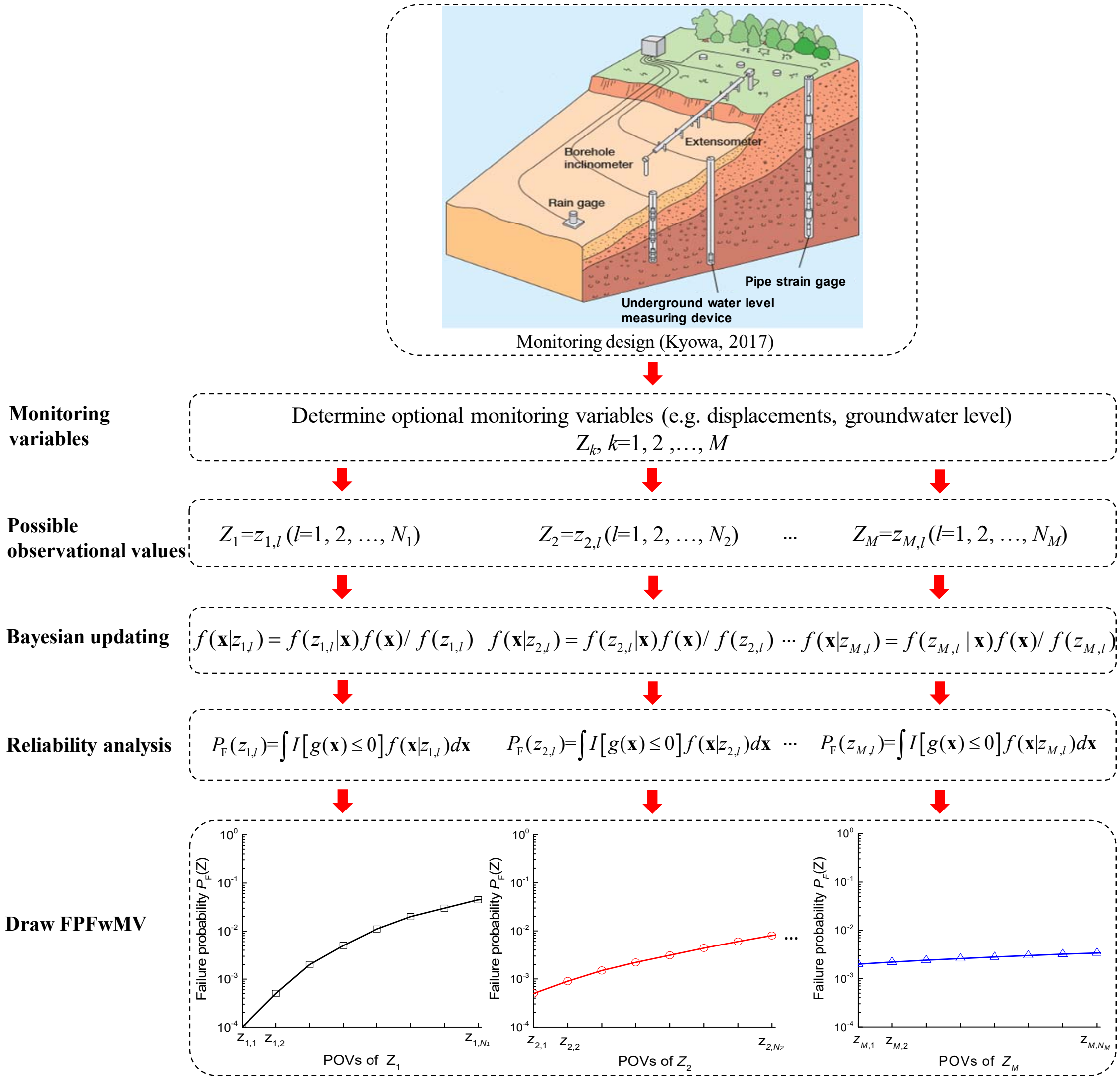


**Fig. 1. Reliability sensitivity analysis framework for monitoring variables**

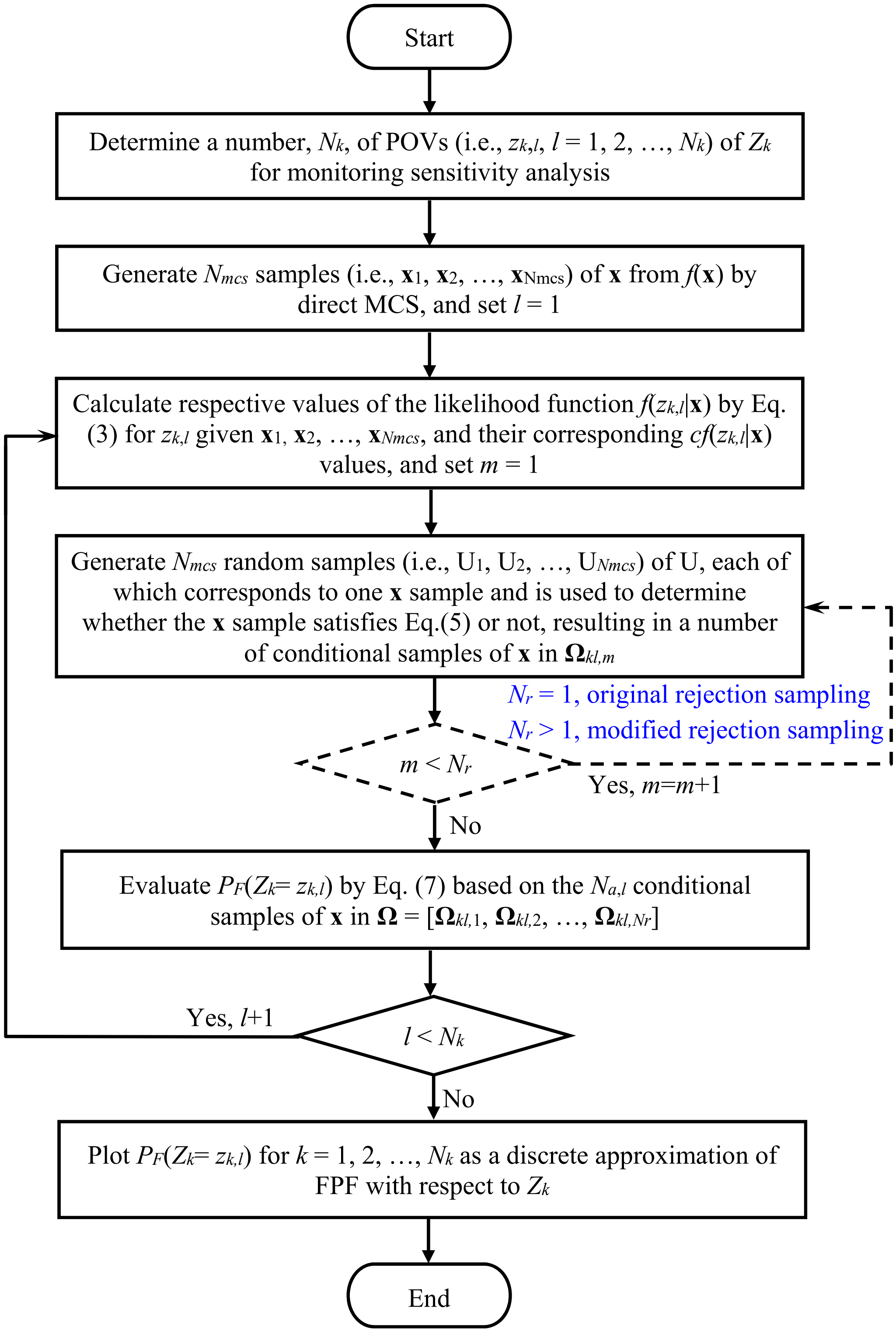


**Fig. 2. Implementation procedure of the proposed sample-based strategy for evaluating FPFwMV**

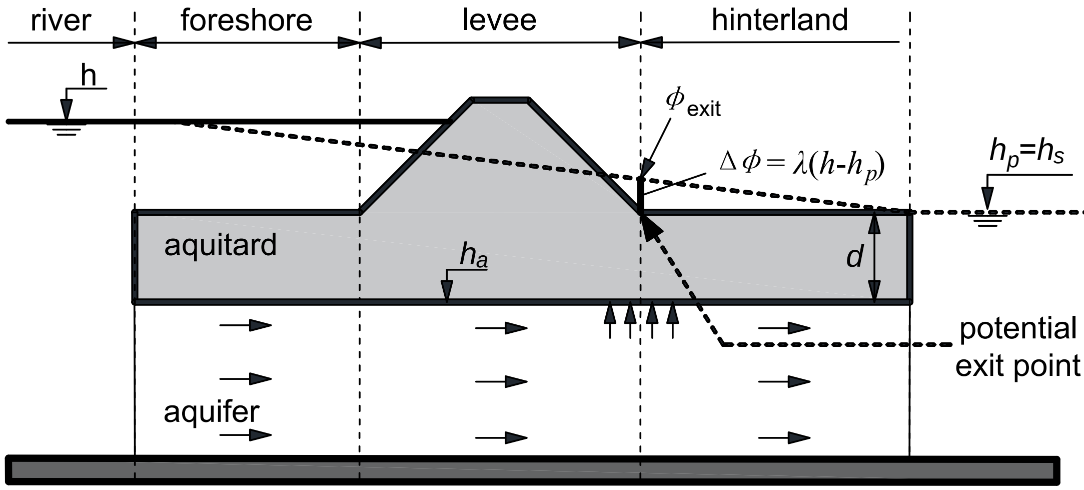


**Fig. 3. The levee head monitoring example (after Schweckendiek and Vrouwenvelder 2013)**

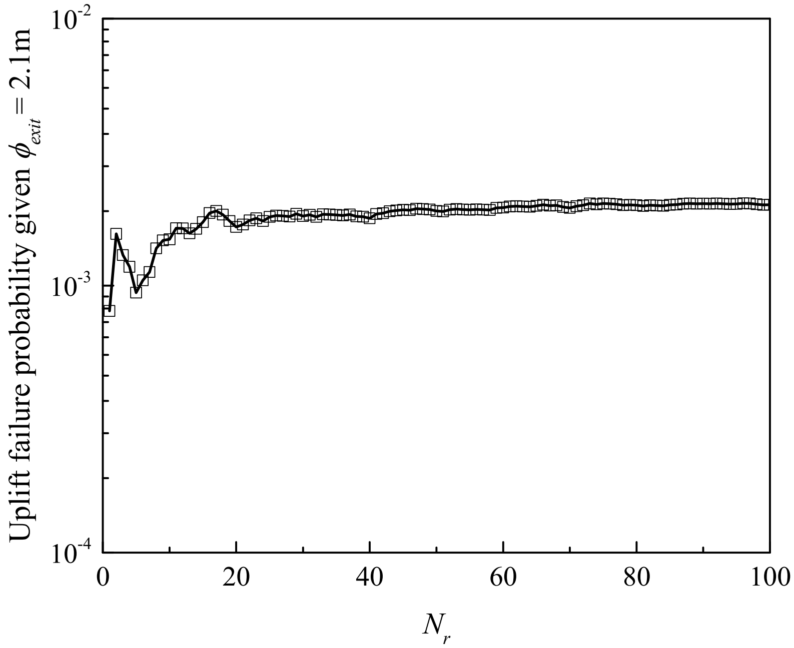


**Fig. 4. Variation of the uplift failure probability given $\phi_{exit}$ = 2.1 m with the increase of $N_r$**

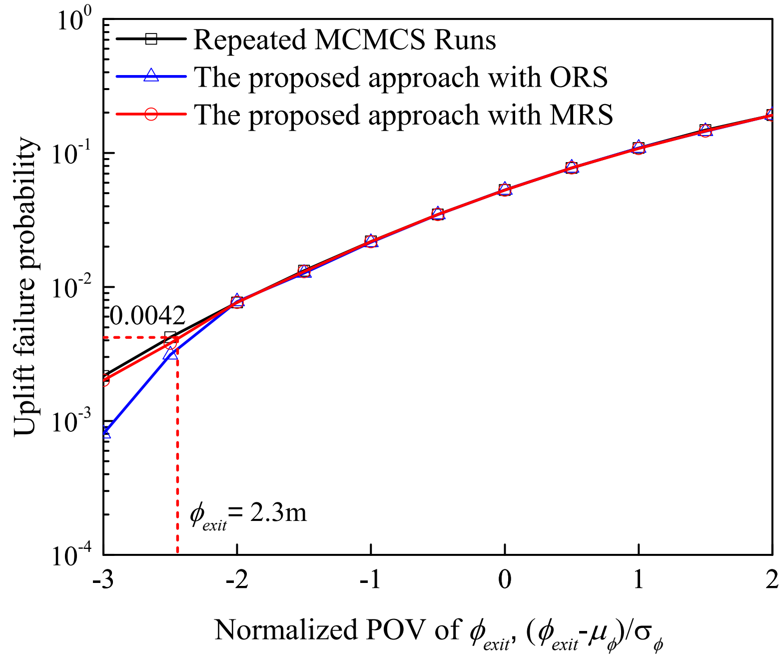


**Fig. 5. Comparison of uplift failure probability functions obtained by different methods**

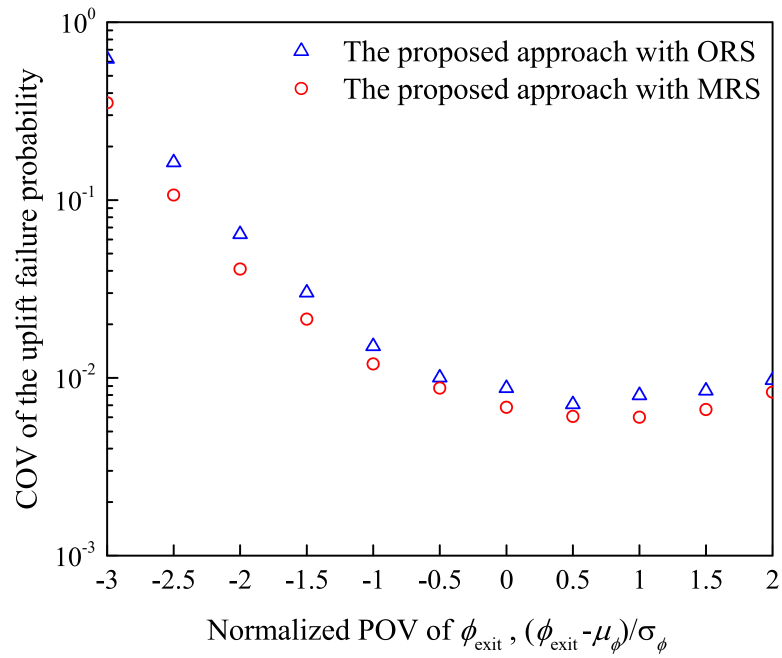


**Fig. 6. Coefficients of variation of uplift failure probabilities calculated by the proposed approach with ORS and MRS**

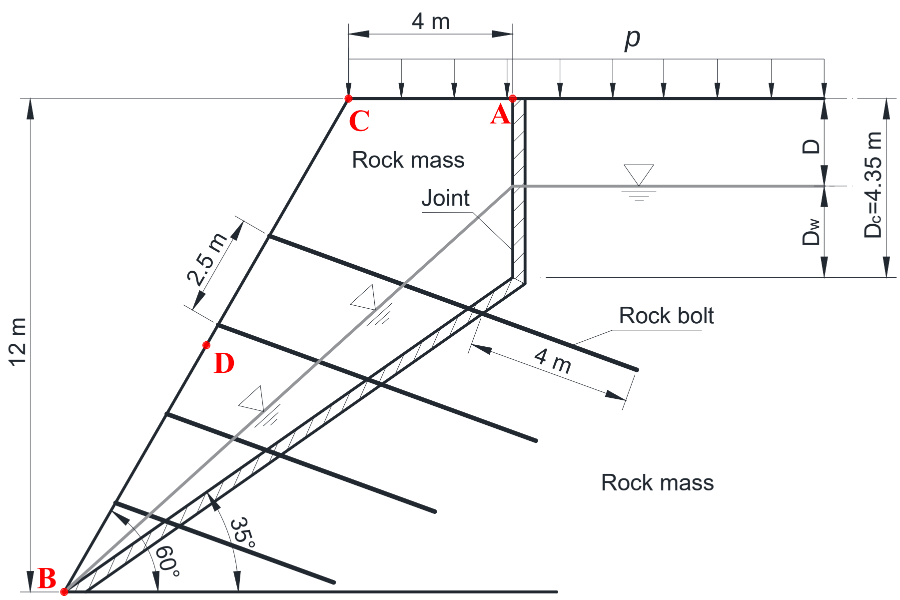


**Fig. 7. Illustration of the rock slope example (after Li et al. 2016c)**

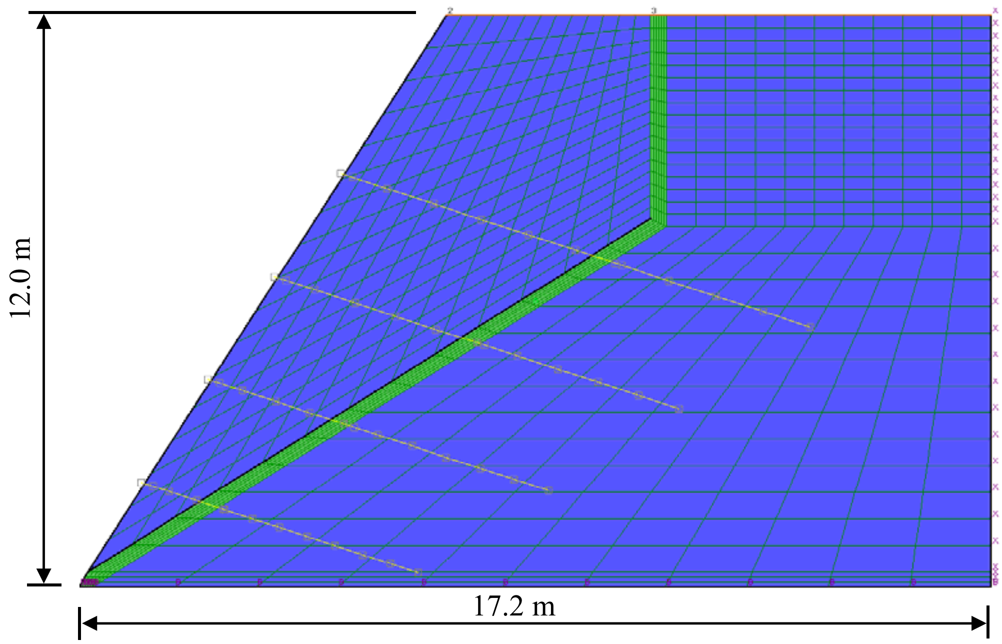


**Fig. 8. The finite difference model for the rock slope example in FLAC 7.0**

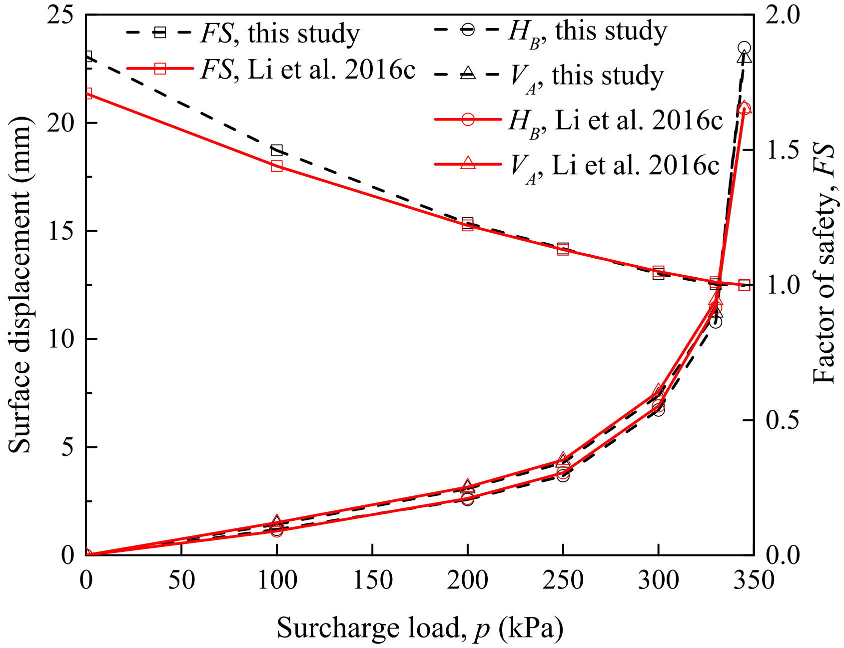


(a) Different surcharge load

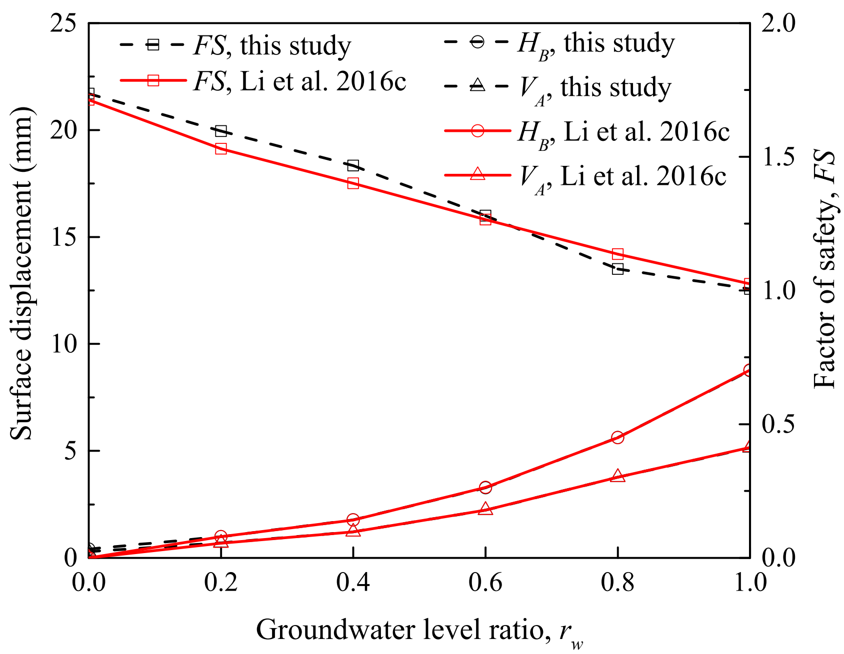


(b) Different groundwater levels

**Fig. 9. Factor of safety and surface displacements at points A and B under different surcharge load and groundwater levels**

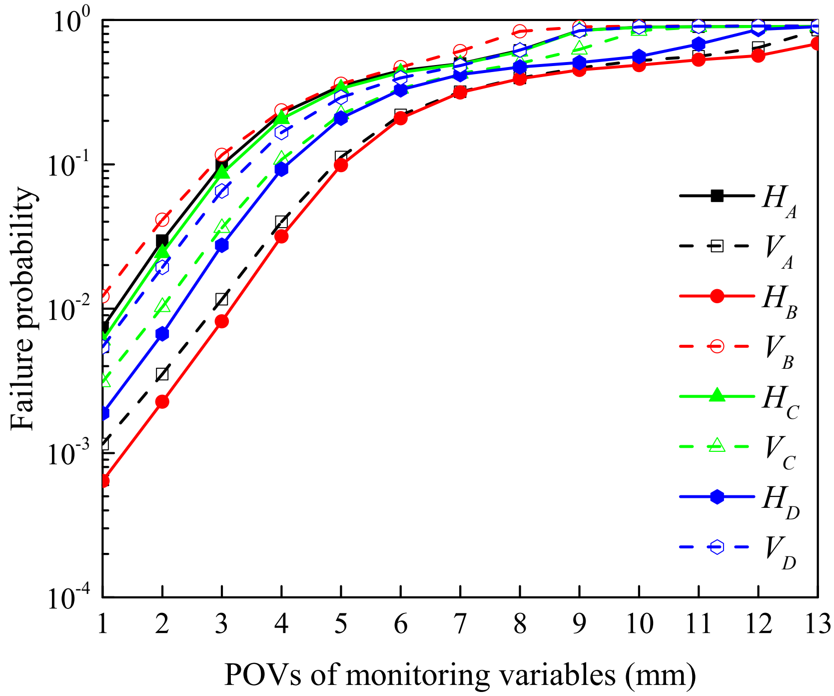


**Fig. 10. Failure probability functions with respect to different monitoring variables in the rock slope example**